Spectroscopic-Grade X-Ray Imaging up to 100-kHz Frame Rate With Controlled-Drift Detectors

Andrea Castoldi, *Member, IEEE*, Chiara Guazzoni, *Member, IEEE*, Pavel Rehak, *Member, IEEE*, and Lothar Strüder

***Abstract*—Controlled-drift detectors are fully depleted silicon detectors for X-ray imaging that combine good position resolution with very fast frame readout. The basic feature of the controlled-drift detector is the transport of the charge packets stored in each pixel column to the output electrode by means of a uniform drift field. The drift time of the charge packet identifies the pixel of incidence. Images of an X-ray source obtained with the controlled-drift detector up to 100-kHz frame rate are presented and discussed. The achievable energy resolution as a function of the operating temperature and frame rate is analyzed.**

***Index Terms*—Controlled-drift detector, fast readout, X-ray imaging.**

I. Introduction

THE controlled-drift detector (CDD) was proposed in 1997 [1], and the first experimental evidence of its working principle was reported in [2]. The device is built on a fully depleted 300-μm-thick high-resistivity wafer and is operated in integrate-readout mode. The basic idea of the CDD is to generate columns of equally spaced potential wells for the electrons by superposing a periodic perturbation of sufficient amplitude to a linear drift potential. During the integration mode, the signal electrons are stored within these wells. The removal of these potential barriers in an externally controlled way allows the use of the linear drift potential to sweep the electrons toward the readout electrodes. The time between the removal of the barriers and the arrival of the signal electrons at the readout electrodes gives the position of the irradiated pixel along the drift direction. The second coordinate is obtained by providing a separate readout electrode for each pixel column. Arrays of deep p-implants provide lateral confinement. In Fig. 1, the layout of the anode region of the controlled-drift detector is shown.

This readout mechanism is inherently faster than the clocked transfer of the rows of pixels toward the readout section typical of the pn charge-coupled device (CCD) because now charge transfer and signal processing are carried out simultaneously. The frame rate in the CDD is ultimately limited by the electron drift time, which is typically 2–6 μs for 1-cm-long device depending on the applied drift field. The advantage of this readout mechanism is twofold: 1) a higher frame rate with respect to the fully depleted pn-CCD [3], which represents the reference device for high-resolution imaging and spectroscopy of X rays, and 2) a lower contribution of the thermal noise due to a shorter integration time, leading to high energy resolution.

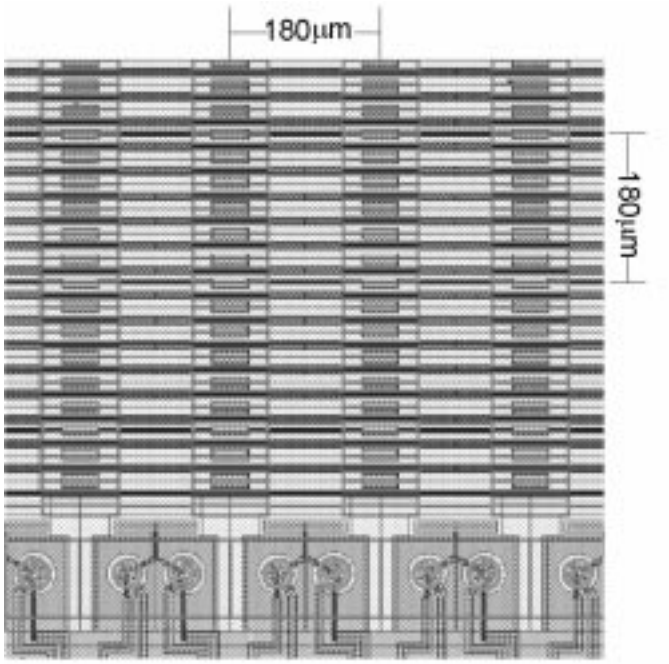

Fig. 1. Layout of the anode region of the controlled-drift detector. The pixel size is also indicated.

We performed the first extended test of the imaging and spectroscopic capability of the CDD by irradiating a column of the detector at room temperature. The aim of the measurements was twofold: 1) verify the proper operation of the CDD at frame frequencies close to the limiting value set by the electron drift time and 2) verify the expected improvement of the energy resolution with the frame frequency. In Section II, we present the images of a ^{55}Fe source obtained with the CDD at different frame rates up to 100 kHz. In Section III, the achievable energy resolution is discussed as a function of the frame rate and of the operating temperature.

II. X-Ray Imaging

One column of the detector has been irradiated with a ^{55}Fe source to verify the imaging capability, the maximum frame

Manuscript received November 3, 2000; revised February 19, 2001. This work was supported by Istituto Nazionale di Fisica Nucleare, Sezione di Milano, and by the U.S. Department of Energy under Contract DE-AC02-98CH10886.

A. Castoldi is with the Dipartimento di Ingegneria Nucleare Ce.S.N.E.F., Politecnico di Milano, Milano 20133, Italy, and INFN, Sezione di Milano, Milano, Italy (e-mail: Andrea.Castoldi@polimi.it).

C. Guazzoni is with the Dipartimento di Elettronica e Informazione, Politecnico di Milano, Milano 20133, Italy, and INFN, Sezione di Milano, Milano, Italy (e-mail: Chiara.Guazzoni@mi.infn.it).

P. Rehak is with the Instrumentation Division, Brookhaven National Laboratory, Upton, NY 11973 USA (e-mail: rehak@klee.inst.bnl.gov).

L. Strüder is with the Halbleiterlabor of the Max Planck Institut, München D-81739, Germany (e-mail: lts@hll.mpg.de).

Publisher Item Identifier S 0018-9499(01)06959-3.

rate, and the achievable energy resolution. The pulses delivered by the on-chip JFET (source follower configuration) were fed to a low-noise voltage preamplifier followed by a pseudo-Gaussian shaper (0.25-μs shaping time) and an 8-bit digitizer controlled by a PC to acquire the output waveforms, subtract the background (mainly due to thermal generation), and compute the amplitude and the drift time of each pulse. We acquired several images of a ^{55}Fe source at room temperature for different frame rates. As the detector area is unshielded, the ratio between the integration time and the readout time is typically chosen greater than one in order to limit the number of out-of-time events. In our case, it was set equal to nine in all measurements. With this choice, we tested the CDD up to a 100-kHz frame rate, corresponding to a duration of the readout phase of 1 μs. Considering that the electron drift occurs within the first 0.7 μs of the readout phase, for the 100-kHz case signal processing was overlapping with the subsequent integration phase.

The operating drift field was 200 V/cm and the amplitude of the surface perturbation was 2 V.

Fig. 2(a) shows the scatter plot energy versus drift time (i.e., position) of the detected events when the CDD is operated at a 10-kHz frame rate. Moving along the time axis, we see that the events are gathered in well-separated clusters centered at about 6 keV (the Mn Kα and Mn Kβ lines are not resolved), indicating the illuminated pixels. In Fig. 2(b), the scatter plot related to a 30-kHz frame rate operation is reported. As we can see, the clusters relative to the Kβ line start to separate from the ones corresponding to the Kα line as the energy resolution is improving. In the image taken at a 100-kHz frame rate [Fig. 2(c)], the Kα and Kβ lines can be clearly distinguished.

A more detailed analysis is obtained by plotting the measured events against one parameter at a time. Fig. 3 shows the distribution of the events along the time axis for the image acquired at a 100-kHz frame rate. The full-width at half-maximum (FWHM) of the peaks is smaller than 15%, leaving a margin for reduction of the pixel size along the drift coordinate (actual size is 180 μm).

Fig. 4 shows the total distribution of the event energies (i.e., the spectrum of the ^{55}Fe source collected by all the pixels) for two different frame rates (10 and 100 kHz).

At a 10-kHz frame rate, the energy resolution at the Mn Kα line (5.899 keV) is 837 eV FWHM, corresponding to an equivalent noise charge (ENC) of 98 electron rms. By increasing the frame frequency, we shorten the integration time and therefore reduce the amount of leakage charge that accumulates in the pixels, thus improving the energy resolution. The energy resolution at 100-kHz frame rate is 339 eV FWHM, corresponding to an ENC of 37 electrons rms.

To further reduce the integration time, we changed the ratio between the duration of the integration and the readout phase. In Fig. 5, the scatter plot energy versus drift time of the detected events when the CDD is operated at a 100-kHz frame rate, with a duration of the integration phase of only 6.7 μs. As expected, we obtained a better energy resolution at the Mn Kα line equal to 296 eV FWHM, corresponding to an ENC of 32 electron rms (see Fig. 6).

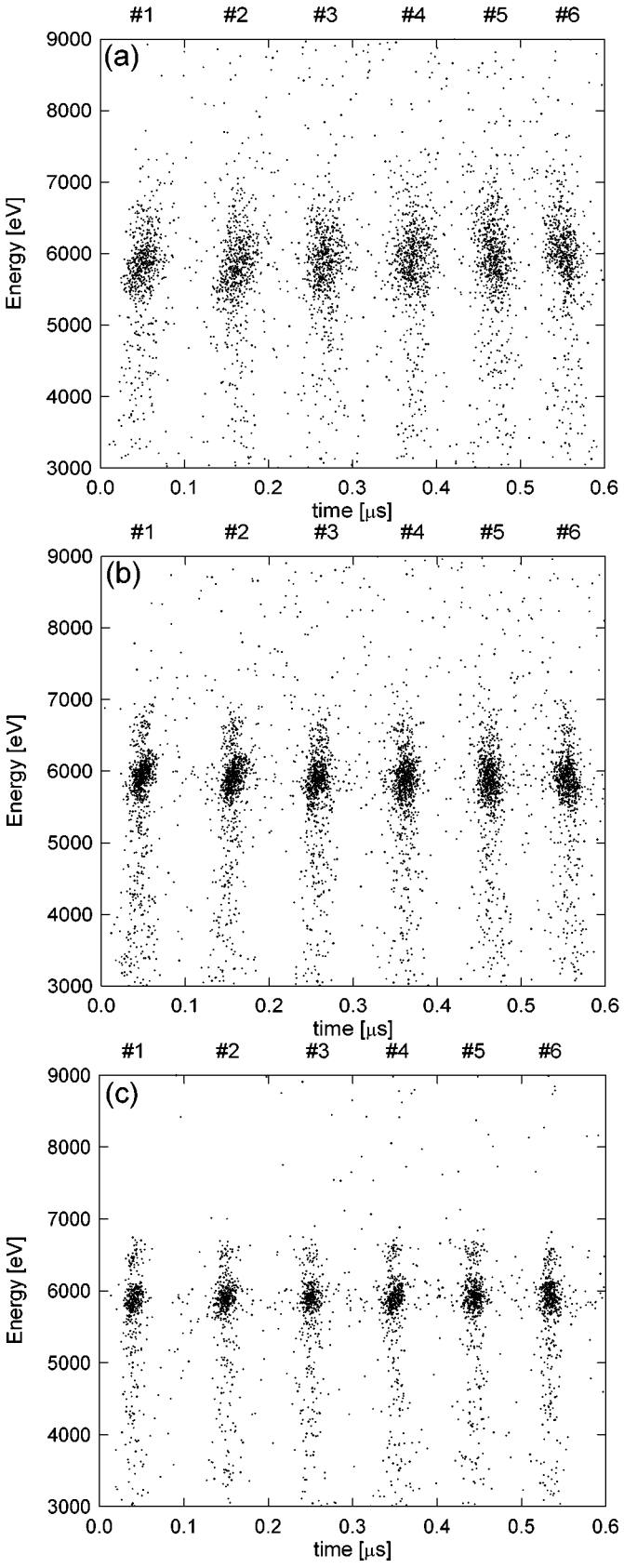

Fig. 2. Scatter plot energy versus drift time of the X-rays of a ^{55}Fe source collected by a column of the CDD. The measurement was carried out at room temperature. The clusters have been labeled with the corresponding pixel numbers. (a) 10-kHz frame rate (integration time 90 μs), (b) 30-kHz frame rate (integration time 30 μs), and (c) 100-kHz frame rate (integration time 9 μs).

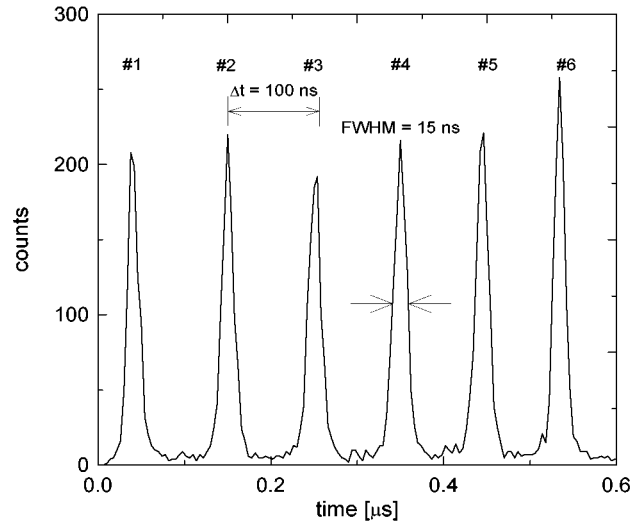

Fig. 3. Distribution of the events of Fig. 2(c) along the drift time (equivalent to the drift coordinate). The pixel number is indicated close to the corresponding peak.

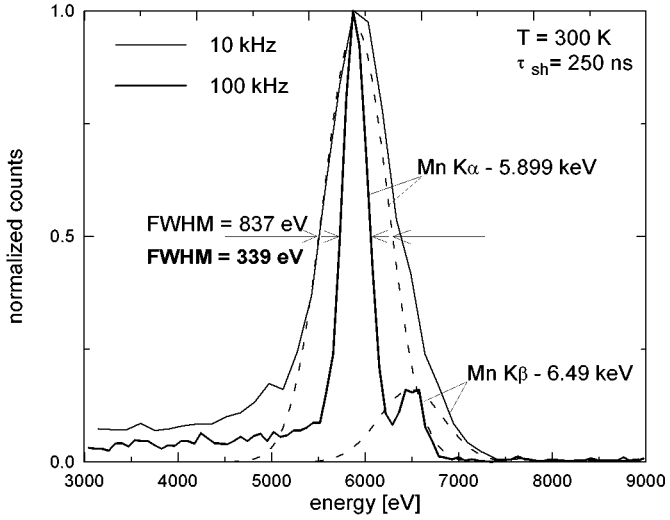

Fig. 4. Distribution of the events of Fig. 2(a) and (c) along the energy. The detector operating temperature is $T = 300$ K and the shaping time is $\tau_{\rm sh} = 250$ ns.

III. Analysis of the Energy Resolution

The readout noise can be expressed in terms of the ENC as

$$\mathrm{ENC}^2 = \mathrm{ENC}_{\rm el}^2 + \mathrm{ENC}_{\rm parallel}^2 + \mathrm{ENC}_{\rm dig}^2. \qquad (1)$$

The noise analysis shows that the contributions are from the noise of the electronic chain ($\mathrm{ENC_{el}} = 20$ electrons rms), the quantization noise of the 8-bit digitizer ($\mathrm{ENC_{dig}} = 12$ electrons rms), and from the parallel noise ($\mathrm{ENC_{parallel}}$) due to the leakage current (about 40 pA/channel) integrated in the pixels during the integration time.

We can model the noise contribution due to the integrated leakage charge as follows. During the integration mode, the leakage current fills the potential wells of the pixels. The average value of the leakage charge in each pixel is equal to

$$Q_L = J_L \cdot A_{\rm pixel} \cdot T_{\rm int} \qquad (2)$$

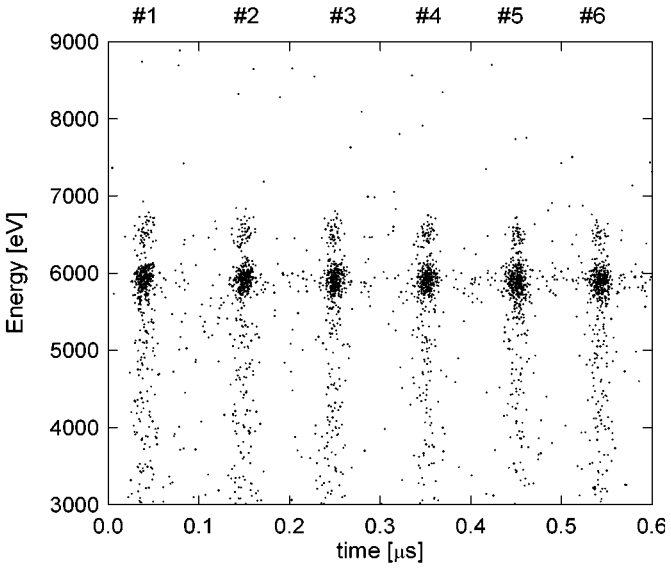

Fig. 5. Scatter plot energy versus drift time of the X-rays of a ^{55}Fe source collected by a column of the CDD at 100-kHz frame frequency. The integration time was set to 6.7 μs and the readout time to 3.3 μs.

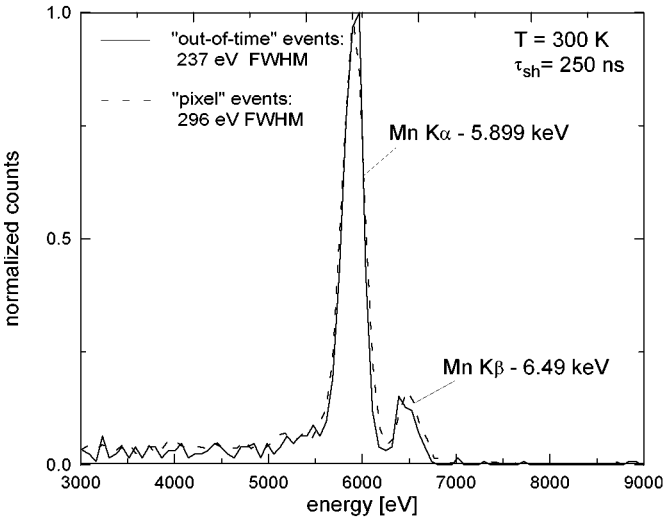

Fig. 6. Comparison of the distribution of the events of Fig. 5 along the energy and of the out-of-time events. The detector operating temperature is $T = 300$ K and the shaping time is $\tau_{\rm sh} = 250$ ns.

where

J_L leakage current per unit area;
$A_{\rm pixel}$ area of one pixel;
$T_{\rm int}$ duration of the integration time.

After the transition to the drift mode, the charges Q_L are released by the pixels and start moving toward the collecting anode. The motion of the integrated charge pulses gives rise to a current pulse that lasts for a time equal to the drift time from the last pixel ($T_{\rm drift_{max}}$) and of average amplitude

$$I_{L,\rm int} = \frac{N_{\rm pixel} \cdot Q_L}{T_{\rm drift_{max}}} = \frac{J_L \cdot N_{\rm pixel} \cdot A_{\rm pixel} \cdot T_{\rm int}}{T_{\rm drift_{max}}} \cong I_L \frac{T_{\rm int}}{T_{\rm drift_{max}}} \qquad (3)$$

where $N_{\rm pixel}$ is the number of pixels in a column and I_L is the leakage current at the anode when the CDD is operated in

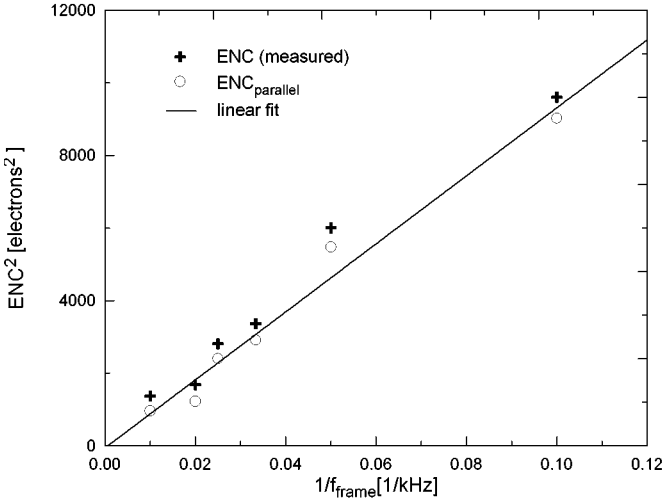

Fig. 7. Measured ENC^2 as a function of the inverse of the frame rate. The derived contribution of the parallel noise is also shown.

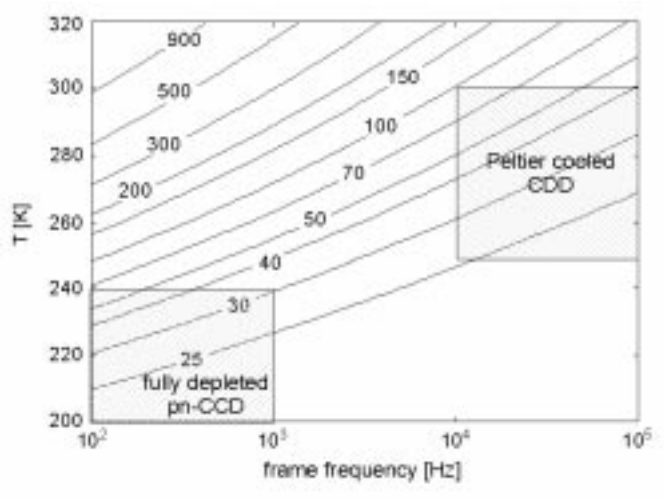

Fig. 8. Contour plot of the achievable energy resolution in terms of ENC as a function of the detector working temperature and of the frame frequency. The ratio between integration time and readout time is set equal to nine.

free-running. The last equality is a slight overestimation due to the fact that I_L also includes the leakage current generated in the anode region. As the drift time from the last pixel ($T_{\mathrm{drift}_{\max}} \cong 0.7\ \mu$s) is greater than the shaping time (0.25 μs), we can estimate the parallel noise contribution ($\mathrm{ENC}^2_{\mathrm{parallel}}$) to the ENC^2 as follows:

$$\mathrm{ENC}^2_{\mathrm{parallel}} = A_3 q I_L \left[1 + \frac{T_{\mathrm{int}}}{T_{\mathrm{drift}_{\max}}}\right] \tau_{\mathrm{sh}} \qquad (4)$$

where

- A_3 shape factor of the filter for parallel noise contribution;
- q electron charge;
- τ_{sh} time constant of the filter.

A first confirmation of the proposed model is given by comparing the energy resolution at the Mn Kα line of the events collected during the integration phase with one of the so-called out-of-time events (i.e., the events hitting the detector during the readout phase and whose position of incidence cannot be determined). The two spectra are compared in Fig. 6 for a frame frequency of 100 kHz and a duration of the integration phase of 6.7 μs. We considered only the out-of-time events hitting the detector in the last 0.3 μs of the readout phase when the leakage current pulse of amplitude $I_{L,\mathrm{int}}$ has expired. The resolution at the Kα line is 237 eV FWHM equal to the resolution achievable with the controlled-drift detector operated in free-running, that is, always in the readout phase.

In Fig. 7, the measured ENC^2 is reported as a function of the inverse of the frame rate. Subtracting quadratically the known contributions of the noise of the electronic chain and the quantization noise from the measured ENC, we calculated the parallel noise contribution. At 10-kHz frame rate, the parallel noise contribution is of 95 electrons, while at 100-kHz frame rate the parallel noise contribution reduces to 31 electrons. From the slope of the fit, we get $I_L = 40$ pA. The plot of ENC^2 as a function of the frame frequency shows good agreement between model and experiment. The spread of the measured points is also related to the approximated energy-voltage calibration factor.

As verified, the increase in the frame rate allows us to reduce significantly the dominant noise contribution of the integrated leakage charge. A well-known way to reduce the thermally generated current is to cool down the detector. In the case of the fully depleted pn-CCDs [3], the only way to reach maximum performances is to cool down the detector, as the duration of the readout time is typically limited to the millisecond range.

The achievable energy resolution, expressed by (1), has been estimated as a function of the operating temperature and of the frame rate. To this end, we assumed that the temperature dependence of the detector leakage current is the same as $n_i^2(T)$ (where $n_i(T)$ is the intrinsic carrier density at temperature T) while the noise contribution of the front-end electronics and of the digitizer was considered constant. Neglecting the increase of the JFET trasconductance at lower temperatures leads to a pessimistic estimate of the energy resolution. The ratio between integration time and readout time is set equal to nine. The equiresolution lines of the estimated ENC in the plane (frame frequency, temperature) are shown in Fig. 8.

IV. Conclusion

In this paper, we presented the first extended characterization of the position-sensing and spectroscopic capabilities of the CDD. One-dimensional images of a ^{55}Fe have been acquired with the CDD operated at room temperature at different frame frequencies up to 100 kHz. The achieved energy resolution at the Mn Kα line and at 100-kHz frame frequency is 339 eV FWHM. The detailed noise analysis that has been presented shows that a dominant contribution to the energy resolution is that of parallel noise. Moreover, the use of a digitizer with a number of bits greater than eight will practically cancel the quantization noise contribution. The possibility to operate the detector at higher frame rates (i.e.,shorter integration times) is equivalent to virtually cooling the detector. As a result, the room-temperature energy resolution approaches the limiting value, obtainable only at cryogenic temperatures if the detector is operated at lower frame rates.

We can expect to achieve energy resolutions close to present state-of-the-art X-ray imagers with more compact Peltier-cooled controlled-drift detector systems.

ACKNOWLEDGMENT

The authors gratefully acknowledge many stimulating discussions with E. Gatti.

REFERENCES

[1] A. Castoldi, C. Guazzoni, A. Longoni, E. Gatti, P. Rehak, and L. Strüder, "Conception and design criteria of a novel silicon device for the measurement of position and energy of X-rays," *IEEE Trans. Nucl. Sci.*, vol. 44, pp. 1724–1732, 1997.

[2] A. Castoldi, E. Gatti, C. Guazzoni, A. Longoni, P. Rehak, and L. Strüder, "The controlled-drift detector," *Nucl. Instrum. Meth.*, vol. A439, pp. 519–528, 2000.

[3] L. Strüder, H. Bräuninger, U. Briel, R. Hartmann, G. Hartner, D. Hauff, N. Krause, B. Maier, N. Meidinger, E. Pfeffermann, M. Popp, C. Reppin, R. Richter, D. Stötter, J. Trümper, U. Weber, P. Holl, J. Kemmer, H. Soltau, A. Viehl, and C. v. Zanthier, "A 36 cm^2 large monolithic pn-charge coupled device X-ray detector for the European XMM satellite mission," *Rev. Sci. Instrum.*, vol. 68, pp. 4271–4274, 1997.